

Topology optimization of viscoelastic microstructures with acoustic impedance manipulation

Hiroaki Deguchi^a, Kei Matsushima^{a,b}, Takayuki Yamada^{a,b,*}

^a*Department of Mechanical Engineering, Graduate School of Engineering, The University of Tokyo, Yayoi 2-11-16, Bunkyo-ku, 113-8656, Tokyo, Japan*

^b*Department of Strategic Studies, Institute of Engineering Innovation, Graduate School of Engineering, The University of Tokyo, Yayoi 2-11-16, Bunkyo-ku, 113-8656, Tokyo, Japan*

Abstract

Mitigating low-frequency noise is particularly challenging due to its limited natural attenuation. This study aims to design viscoelastic composite microstructures that achieve both low acoustic reflection and high internal damping by simultaneously optimizing their effective acoustic impedance and attenuation characteristics. Using homogenization theory and density-based topology optimization, viscoelastic and impedance-matching materials are distributed within a unit cell to manipulate these properties. Numerical results show that optimized microstructures with viscoelastic lattice embedded in impedance-matching material outperform pure viscoelastic materials in attenuation while maintaining low reflection. This demonstrates the potential of microstructural engineering for effective low-frequency noise mitigation.

Keywords: Viscoelasticity, Topology optimization, Acoustic impedance, Homogenization method, Adjoint variable method, Wave attenuation

1. Introduction

Low-frequency noise, typically defined as sound with a frequency below 100 Hz, is a pervasive environmental issue originating from sources such as heavy machinery, transportation systems, and industrial activities [1]. Its long wavelength allows it to propagate over extensive distances with low

*Corresponding author

Email address: t.yamada@mech.t.u-tokyo.ac.jp (Takayuki Yamada)

attenuation, leading to significant physical disturbances such as structural vibrations and adverse psychological and physiological effects on humans [2]. Traditional noise control strategies often rely on sound absorption, converting acoustic energy into heat, or sound insulation, which aims to block sound transmission [3].

This study specifically targets the challenge of mitigating low-frequency sound. Impedance-matching materials, often realized as lightweight porous structures, play a crucial role by minimizing reflections at the material-air interface; achieving an acoustic impedance close to that of air is key to reducing this reflection [4, 5, 6]. However, for low-frequency sound, these materials typically require substantial thickness to be effective and may still suffer from significant sound transmission if they lack inherent dissipative mechanisms [7]. While techniques such as adding air gaps or layering materials can enhance performance, they often introduce practical limitations, e.g., increased bulk and complexity [5, 7]. Another approach involves viscoelastic materials, which dissipate acoustic energy internally as heat due to their inherent damping properties, thus reducing transmitted sound [8, 9, 10]. Time-harmonic oscillation of viscoelastic materials is characterized by complex-valued, frequency-dependent elastic moduli, where the imaginary part (loss modulus) directly governs energy dissipation [8, 9, 10]. The challenge, however, is that viscoelastic materials often present a significant impedance mismatch with air, leading to strong reflections.

The inherent trade-off between the low reflection of impedance-matching materials and the high internal damping of viscoelastic materials motivates the exploration of viscoelastic composite microstructures. This research posits that by strategically engineering the microscopic arrangement of these two constituent materials, it is possible to create a composite that synergistically combines low reflectivity with high sound attenuation. To design such microstructures effectively, particularly for low frequencies where wavelengths are much larger than the microstructural scale, the homogenization method based on two-scale asymptotic expansions provides a powerful analytical tool [11, 12]. This method allows for the derivation of effective macroscopic properties from the microstructural details, even when material properties are complex-valued, by formally extending the standard elastostatic framework [13]. Seminal work by Yi et al. [14] specifically addressed the homogenization of viscoelastic composites.

To systematically design these microstructures, topology optimization has emerged as a powerful computational tool [15]. This method opti-

mizes material layout within a given design domain to achieve superior performance. Among various approaches, density-based methods, particularly the Solid Isotropic Material with Penalization (SIMP) scheme [16, 17], have been widely adopted for their simplicity and effectiveness in diverse applications such as compliant mechanism design [18] and multiphysics systems [19, 20]. When combined with homogenization, topology optimization becomes a promising strategy for designing material microstructures with desired macroscopic properties [21, 22, 23]. This multiscale approach has enabled the design of novel materials and metamaterials with extraordinary characteristics in acoustics [24, 25]. Previous studies have explored topology optimization for maximizing damping in viscoelastic structures [26, 27] and have notably addressed the homogenization of viscoelastic composites for optimization purposes [28, 29, 30], building upon a foundation of viscoelastic homogenization [14]. Extending these optimization frameworks to explicitly incorporate acoustic impedance control is therefore anticipated to enable the design of microstructures with enhanced acoustic performance, achieving both low reflection and high attenuation.

This study aims to minimize sound reflection and maximize internal attenuation in viscoelastic composites by simultaneously controlling their effective acoustic impedance and damping via the homogenization method and topology optimization. Effective acoustic impedance and the imaginary part of the wavenumber, evaluated through homogenization of the viscoelastic composite’s microstructure, are then incorporated into an objective function for topology optimization. The proposed method provides a design framework for lightweight, thin, and highly effective acoustic materials for low-frequency noise control.

The remainder of this paper is organized as follows. Section 2 describes the design problem, the governing equations for the acoustic and viscoelastic fields, and the derivation of effective properties using the homogenization method. Section 3 explains the formulation of the topology optimization problem, sensitivity analysis, and the optimization algorithm. Section 4 presents numerical examples to validate the effectiveness of the proposed method. Finally, Section 5 concludes the paper.

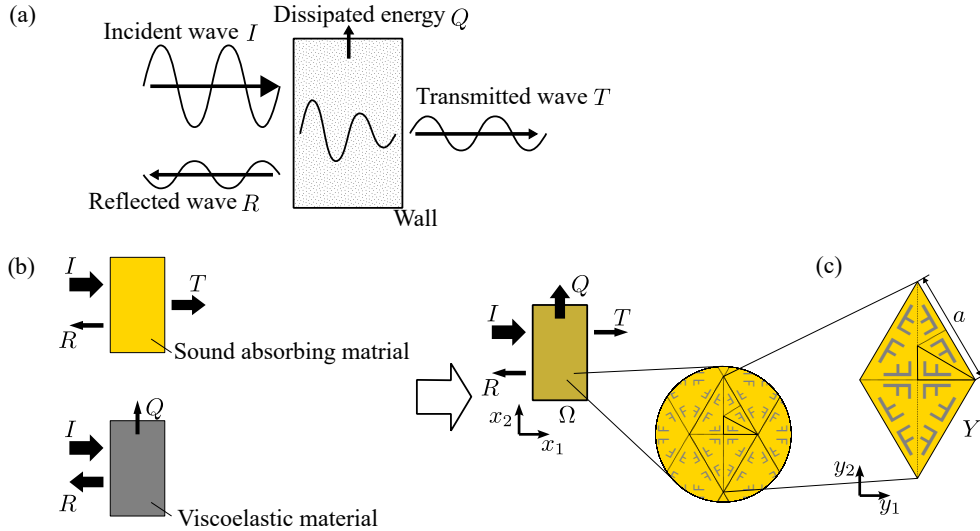


Figure 1: Model of a low-reflection and high-damping structure. (a) Illustration of the design problem. (b) Schematic of the viscoelastic composites. (c) The unit cell comprises two phases: impedance-matching material and viscoelastic material. The periodic structure is homogenized in the limiting case $a \rightarrow 0$.

2. Model

2.1. Design problem for a low-reflection and high-damping structure

First, we consider the design of a structure that simultaneously exhibits low reflection and high damping characteristics for incident sound waves. Our aim is to minimize the energy reflected from the structure's front surface and the energy transmitted through its entirety. As depicted in Figure 1(a), an incident sound wave with energy I impinges upon a structure. This interaction results in a reflected wave with energy R and a transmitted wave with energy T . Within the structure, a portion of the sound energy, Q , is dissipated, typically as heat, due to the material's damping properties. Effective acoustic design, therefore, seeks to minimize the reflection coefficient (R/I) and the transmission coefficient (T/I).

In pursuit of this goal, a fundamental trade-off often arises when considering single-phase materials. On one hand, an impedance-matching material can be designed to have an acoustic impedance close to that of the surrounding medium (e.g., air). As illustrated conceptually in Figure 1(b) (top left), this minimizes the impedance mismatch at the interface, leading to a

small reflection coefficient (R/I). However, such materials, if they are not inherently highly dissipative (e.g., lightweight porous materials), may allow a significant portion of the non-reflected energy to pass through, resulting in a large transmission coefficient (T/I).

On the other hand, a viscoelastic material is characterized by its ability to dissipate mechanical energy internally. As shown in Figure 1(b) (bottom left), if a structure is made solely of a highly dissipative viscoelastic material, it can significantly attenuate the wave as it propagates, leading to a small transmission coefficient (T/I). However, viscoelastic materials often have acoustic impedances that are substantially different from that of air, causing a significant impedance mismatch at the incident surface and thus a large reflection coefficient (R/I).

This apparent conflict between minimizing reflection and maximizing internal attenuation suggests that neither material type alone is optimal for achieving both objectives simultaneously. Therefore, this study explores the potential of viscoelastic composite microstructures, as schematically shown in Figure 1(b) (right). By strategically combining an impedance-matching material and a viscoelastic material at the microstructural level, we hypothesize that it is possible to engineer a composite that synergistically leverages the strengths of both constituents. The aim is to create a material that not only presents a favorable impedance to the incident wave, thereby reducing reflections, but also possesses enhanced internal damping mechanisms to absorb the energy that does enter, thus minimizing transmission. The design of such a composite microstructure is the central focus of this work.

2.2. Formulation of the design problem

We now derive the quantitative conditions for minimizing reflected and transmitted waves, which were qualitatively discussed as the objectives in Section 2.1.

As shown in Figure 2, we consider the left half-plane Ω_0 filled with air and the right half-plane Ω_1 occupied by a viscoelastic material.

We assume that the acoustic pressure field $\tilde{p}(x, t)$ in the sound domain takes the time-harmonic form $\tilde{p}(x, t) = p(x)e^{-i\omega t}$, where ω is the angular frequency. Under this assumption, the governing equation of the acoustic pressure $p(x)$ in air is given by the Helmholtz equation:

$$\nabla^2 p(x) + k_0^2 p(x) = 0 \quad \text{in } \Omega_0, \quad (1)$$

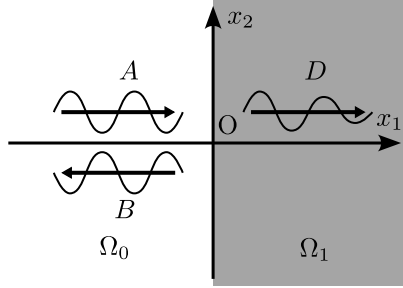


Figure 2: Half-plane of the sound field and the viscoelastic field.

where $k_0 = \omega/c_0$ is the wavenumber in air, and $c_0 = \sqrt{\kappa_0/\rho_0}$ is the speed of sound, with κ_0 and ρ_0 denoting the bulk modulus and mass density of air, respectively.

Similarly, we assume that the displacement field $\tilde{\mathbf{u}}(x, t)$ in the viscoelastic domain takes the time-harmonic form $\tilde{\mathbf{u}}(x, t) = \mathbf{u}(x)e^{-i\omega t}$. Under the plane-strain condition, the governing equation for the viscoelastic field can be expressed as:

$$\operatorname{div}(C : \varepsilon(\tilde{\mathbf{u}}(x))) + \rho_1 \omega^2 \tilde{\mathbf{u}}(x) = 0 \quad \text{in } \Omega_1. \quad (2)$$

where the elasticity tensor C can be expressed using the Lamé constants λ and μ as follows:

$$C_{ijkl} = \lambda \delta_{ij} \delta_{kl} + \mu (\delta_{ik} \delta_{jl} + \delta_{il} \delta_{jk}), \quad (3)$$

where δ_{ij} is the Kronecker delta, and the Lamé constants are expressed using complex Young's modulus $E = E_1 + iE_2$ and Poisson's ratio ν as follows:

$$\lambda = \frac{E\nu}{(1+\nu)(1-2\nu)}, \quad \mu = \frac{E}{2(1+\nu)}. \quad (4)$$

The strain tensor $\varepsilon(\mathbf{u})$ can be associated with the displacement \mathbf{u} as follows:

$$\varepsilon_{ij} = \frac{1}{2} \left(\frac{\partial u_j}{\partial x_i} + \frac{\partial u_i}{\partial x_j} \right). \quad (5)$$

The density of the viscoelastic material is denoted as ρ_1 .

The stress tensor $\boldsymbol{\sigma}$ is given by $\sigma_{ij} = C_{ijkl} \varepsilon_{kl}$.

Boundary conditions at the interface between the sound field and the viscoelastic field are imposed as follows:

$$-p\mathbf{n} = \boldsymbol{\sigma} \cdot \mathbf{n} \quad \text{on } \Gamma, \quad (6)$$

$$\frac{1}{\rho_0\omega^2}\nabla p \cdot \mathbf{n} = \mathbf{u} \cdot \mathbf{n} \quad \text{on } \Gamma, \quad (7)$$

where \mathbf{n} is the unit normal vector on the boundary Γ between the sound field and the viscoelastic field. Without loss of generality, Γ lies along the line $x_1 = 0$, and the unit normal vector \mathbf{n} is defined as $(1, 0)$.

We consider an incident sound wave with amplitude A propagating in the positive x_1 direction in Ω_0 , which generates a reflected sound wave with amplitude B and a transmitted P-wave with amplitude D in the viscoelastic material, as shown in Figure 2. Furthermore, we impose the radiation condition at a sufficiently far distance from the interface. In this case, the sound pressure p and the displacement field \mathbf{u} that satisfy the governing equations (1) and (2) and the boundary conditions (6) and (7) can be expressed as follows:

$$p(x) = A \exp(ik_0x_1) + B \exp(-ik_0x_1) \quad \text{in } \Omega_0, \quad (8)$$

$$u_1(x) = ik_1D \exp(ik_1x_1) \quad \text{in } \Omega_1, \quad (9)$$

$$u_2(x) = 0 \quad \text{in } \Omega_1, \quad (10)$$

where $k_1 = \omega/c_1 \in \mathbb{C}$ is the wavenumber, and $c_1 = \sqrt{(\lambda + 2\mu)/\rho_1}$ is the speed of P-wave in the viscoelastic material. The coefficients A , B , and D satisfy the following relationships:

$$A + B = \rho_1\omega^2D, \quad (11)$$

$$A - B = \rho_0\omega^2\frac{c_0}{c_1}D. \quad (12)$$

The reflection coefficient R/I can be expressed as follows:

$$\frac{R}{I} = \left| \frac{B}{A} \right|^2 = \left| \frac{\rho_1c_1 - \rho_0c_0}{\rho_1c_1 + \rho_0c_0} \right|^2. \quad (13)$$

The qualitative discussion in Section 2.1 regarding the dual objectives of low reflection and high attenuation can now be translated into quantitative targets based on the properties of the homogenized material. First, we aim to

minimize the reflected wave, which requires reducing the absolute difference between the acoustic impedances $\rho_1 c_1$ and $\rho_0 c_0$, as shown in Eq. (13). Second, the attenuation characteristics of the viscoelastic material are enhanced when the imaginary part of the complex wavenumber $\text{Im}[k_1]$ becomes larger, as shown in Eq. (9).

2.3. Homogenization for viscoelastic microstructures

In this section, we employ a homogenization method based on the two-scale asymptotic expansion technique to determine the effective properties of viscoelastic microstructures comprising a periodic lattice with two phases. The viscoelastic nature of the materials implies that their mechanical properties, such as the elasticity tensor C and Lamé parameters, are complex-valued and frequency-dependent. However, the mathematical framework of homogenization theory can be formally extended to such complex-valued coefficients, treating them similarly to real-valued coefficients in standard elastostatics [13, 31]. This allows us to derive effective complex-valued homogenized properties for the composite.

The system of composite materials occupies a domain Ω , which consists of a periodic array of unit cells. In the region Ω , unit cell regions Y with a characteristic side length a are arranged in a honeycomb lattice, as shown in Figure 1(b), (c), and each unit cell is composed of two types of homogeneous materials: impedance-matching material and viscoelastic material. Here, since the discussion in Section 2.2 assumes an effectively isotropic behavior for the homogenized material, we consider a lattice structure with symmetry in the honeycomb lattice to ensure that the homogenized material tensor can be characterized as isotropic, described by only two independent complex Lamé constants. The basic translation vectors that define the periodic lattice of these unit cells are denoted by $a\hat{e}_1$ and $a\hat{e}_2$, where \hat{e}_1 and \hat{e}_2 are unit vectors.

In this system, the displacement field in the region Ω is represented by the solution of the elastodynamic problem, denoted by $\mathbf{u}_a(x)$, as shown below:

$$\begin{cases} \text{div} \left(C \left(\frac{x}{a} \right) \nabla \mathbf{u}_a \right) + \rho \left(\frac{x}{a} \right) \omega^2 \mathbf{u}_a = 0 & \text{in } \Omega \\ \mathbf{u}_a = 0 & \text{on } \partial\Omega \end{cases} \quad (14)$$

where the variable $x \in \mathbb{R}^2$ represents the macro-scale coordinates, and $y = x/a$ represents the micro-scale oblique coordinates normalized by the unit cell size a . The fourth-order elasticity tensor $C(y)$ and density $\rho(y)$ are Y -periodic. Namely, for the basis vectors \hat{e}_1 and \hat{e}_2 , the coefficients satisfy the

following periodicity condition:

$$C(y + \hat{e}_i) = C(y), \quad \rho(y + \hat{e}_i) = \rho(y) \quad (i = 1, 2). \quad (15)$$

We use a homogenization method to characterize the periodic array as a homogenized viscoelastic microstructure. When the unit cell size a is sufficiently small compared to the wavelength, the homogenized elasticity tensor C_{ijkl}^H and density ρ^H can be characterized as follows:

$$C_{ijkl}^H = \int_Y (g_{ij} + \varepsilon(\chi_{ij})) : C : g_{kl} dy, \quad (16)$$

$$\rho^H = \frac{1}{|Y|} \int_Y \rho(y) dy, \quad (17)$$

where $|Y|$ is the volume of the unit cell, and the second-order tensor g is defined by $g_{ij} = \frac{1}{2} (\hat{e}_i \otimes \hat{e}_j + \hat{e}_j \otimes \hat{e}_i)$, and χ_{ij} are solutions of the following unit cell problem:

$$\begin{cases} -\operatorname{div}(C : \varepsilon(\chi_{ij})) = \operatorname{div}(C : g_{ij}) & \text{in } Y, \\ y \mapsto \chi_{ij}(y) & Y\text{-periodic} \end{cases} \quad (18)$$

for each $i, j = 1, 2$.

3. Topology optimization

This section is devoted to a density-based topology optimization method for the design problem described in Section 2.1. We first formulate our topology optimization problem and subsequently explain its sensitivity analysis with an algorithm for the topology optimization.

3.1. Formulation of topology optimization problem

A two-phase topology optimization based on the Solid Isotropic Material with Penalization (SIMP) method [17, 20] is used to solve the structural optimization problem in the unit cell Y . A density function $\theta : Y \rightarrow [0, 1]$ is defined in the unit cell Y to represent the material distribution of the viscoelastic material. The elasticity tensor $C(y)$ and density $\rho(y)$, which depend on the density function θ , are expressed as follows:

$$C(y) = \theta(y)^3 C_1 + (1 - \theta(y)^3) C_2, \quad (19)$$

$$\rho(y) = \theta(y)^3 \rho_1 + (1 - \theta(y)^3) \rho_2, \quad (20)$$

where C_1 and ρ_1 are the elasticity tensor and density of the viscoelastic material, and C_2 and ρ_2 are those of the impedance-matching material.

The objective is to find a density function θ such that it minimizes the reflection coefficient R/I and maximizes the imaginary part of the complex wavenumber $\text{Im}[k_1]$. The objective functional $J(\theta)$ is defined as follows:

$$J(\theta) = b_1 J_1(\chi_{ij}(\theta)) + b_2 J_2(\chi_{ij}(\theta)), \quad (21)$$

$$J_1 = \left(1 - \left| 1 - \frac{\sqrt{\kappa_0 \rho_0}}{\sqrt{(\lambda_\theta^H + 2\mu_\theta^H) \rho_\theta^H}} \right|^2 \right)^2, \quad (22)$$

$$J_2 = \sqrt{\frac{\kappa_0}{\rho_0}} \left| \text{Im} \left[\sqrt{\frac{\rho_\theta^H}{\lambda_\theta^H + 2\mu_\theta^H}} \right] \right|, \quad (23)$$

where b_1 and b_2 are the weights of the objective functionals, λ_θ^H and μ_θ^H are the Lamé constants derived from the homogenized elasticity tensor C_θ^H , and ρ_θ^H is the homogenized density. The first term J_1 is formulated to promote impedance matching, and the second term J_2 represents a scaled version of the imaginary part of the complex wavenumber in the homogenized viscoelastic medium, which relates to attenuation. The squaring in J_1 makes deviations of its base term (which represents non-reflection and ideally equals 1) from this target value more pronounced in the derivative, thereby more effectively pulling the optimization towards this goal.

The optimization problem can be expressed as follows:

$$\max_{\theta} J(\chi_{ij}(\theta)) \quad (24)$$

$$\text{subject to } \int_Y \theta(y) dy - V_1^{\max} \leq 0, \quad (25)$$

where V_1^{\max} is the maximum volume fraction of the viscoelastic material in the unit cell Y .

3.2. Sensitivity analysis

The derivative of the objective functional $J(\theta)$ with respect to the density function θ is called the sensitivity of the objective functional. The sensitivity of the objective functional is calculated using the adjoint variable method [31]. As discussed in Section 2.3, the objective functional $J(\theta)$ is expressed as a function of the homogenized elasticity tensor C_θ^H and density ρ_θ^H ; thus,

it is necessary to calculate the derivatives of these homogenized properties with respect to the density function θ . Using the adjoint variable method, the derivatives of the homogenized elasticity tensor and density with respect to θ can be obtained as follows:

$$dC_{ijkl}^H(\theta)[\tilde{\theta}] = \int_Y (g_{ij} + e(\chi_{ij}(\theta))) : dC(\theta)[\tilde{\theta}] : (g_{kl} + e(\chi_{kl}(\theta))) dy, \quad (26)$$

$$d\rho_\theta^H[\tilde{\theta}] = \frac{1}{|Y|} \int_Y d\rho_\theta[\tilde{\theta}] dy, \quad (27)$$

where $dF(\theta)[\tilde{\theta}]$ denotes the derivative of functional F with respect to the direction $\tilde{\theta}$ at θ , i.e.,

$$F(\theta + \tilde{\theta}) = F(\theta) + dF(\theta)[\tilde{\theta}] + o(\|\tilde{\theta}\|). \quad (28)$$

3.3. Optimization algorithm

In this study, the optimization algorithm is based on the following steps:

step 1 : Initialize the density function θ .

step 2 : Solve the unit cell problem (18) to obtain $\chi_{ij}(\theta)$.

step 3 : Calculate the homogenized elasticity tensor C_θ^H , density ρ_θ^H and the objective functional $J(\theta)$.

step 4 : Compute the update direction $\tilde{\theta}$ of the objective functional $J(\theta)$ using the derivatives obtained from Eqs. (26) and (27) via the chain rule.

step 5 : Update the density function as $\theta \leftarrow \theta + \alpha\tilde{\theta} + \lambda_1$, where α is the step size and λ_1 is the Lagrange multiplier for the volume constraint.

step 6 : Return to step 2 until the convergence condition is satisfied.

The open-source finite element method solver FreeFEM++ [32] is used to perform the finite element analysis and sensitivity calculations.

4. Numerical examples

In this section, we present numerical examples to demonstrate the effectiveness of the proposed method. The parameters used in the numerical examples are listed in Table 1. Note that the complex Young’s modulus of the viscoelastic materials is frequency-dependent; hence, the parameter values are specified at the frequency indicated by ω in Table 1. The density of air is set to $\rho_0 = 1.2\text{kg/m}^3$, and the bulk modulus of air is set to $\kappa_0 = 1.4 \times 10^5\text{Pa}$.

Table 1: Physical properties of each material.

Material	ω (rad/s)	E (Pa)	ν	ρ (kg/m ³)
Epoxy	0.5	$1.71 \times 10^9 - 1.14 \times 10^9i$	0.35	1850
Sponge	All	5.0×10^6	0.11	20

In the optimization, the maximum volume fraction of the viscoelastic material is set to 0.1. The weights of the two objective functionals are set to $b_1 = 1.0 \times 10^6$ and $b_2 = 1.0 \times 10^{-5}$, respectively. Since the objective functionals J_1 and J_2 are formulated to be dimensionless, the weights b_1 and b_2 are also dimensionless.

4.1. Optimized design

Figure 3 shows the optimization process from the initial structure to the optimized structure. The initial structure has a volume fraction of 0.04 for the viscoelastic material, which is discretely scattered and disconnected within the unit cell. The volume fraction of the viscoelastic material increased and decreased during the optimization process, ultimately reaching 0.086, which satisfies the volume constraint.

The results show that the reflection coefficient cannot be reduced below the performance of the impedance-matching material alone, while the attenuation characteristics exceeded those of the viscoelastic material alone. The optimized structure is composed mostly of impedance-matching material, with the viscoelastic material forming a connected structure. Using this optimized structure, we can reduce the reflected wave while increasing the attenuation, effectively eliminating low-frequency noise. Furthermore, the optimization results suggest a design strategy for achieving both low reflection and high attenuation. Specifically, this can be realized by increasing

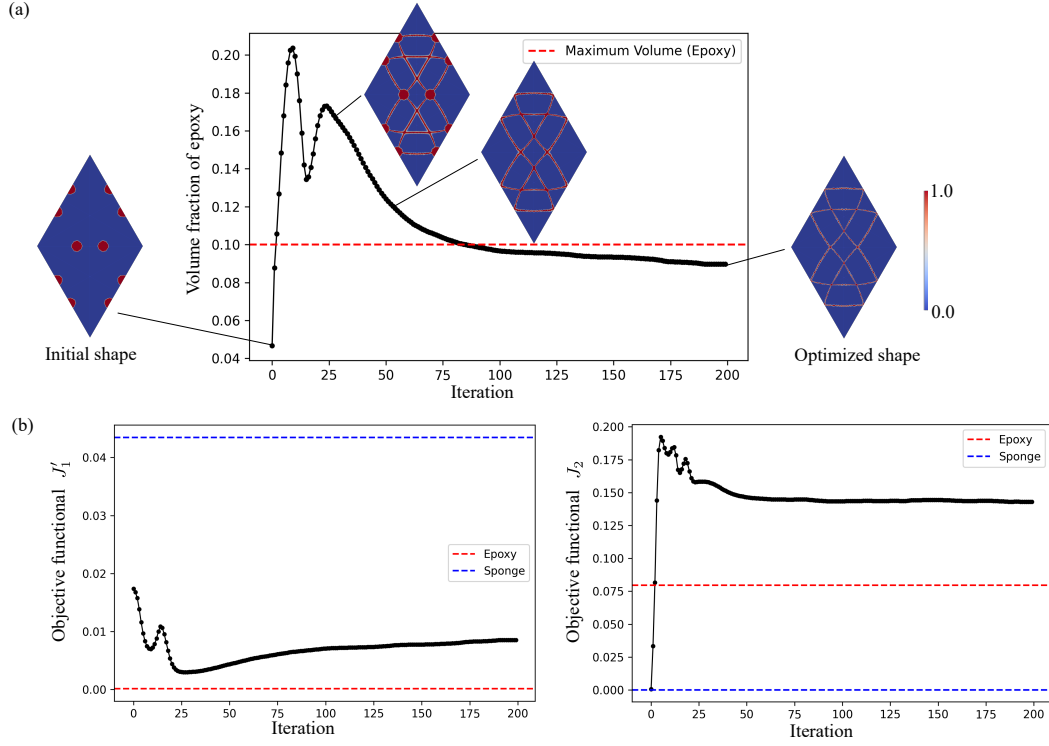


Figure 3: Histories of the optimized design process. (a) History of the volume fraction of the viscoelastic material and unit cell designs at steps 0, 25, 50, and 199. (b) History of the objective functional $J_1 := 1 - \left| 1 - \frac{\sqrt{\kappa_0 \rho_0}}{\sqrt{(\lambda_\theta^H + 2\mu_\theta^H) \rho_\theta^H}} \right|$ and J_2 .

the volume fraction of the impedance-matching material and embedding the viscoelastic material in a network-like configuration throughout the absorber.

5. Conclusion

In this study, we proposed a topology optimization method for viscoelastic composites to minimize the reflected and transmitted waves.

We derived expressions for the effective acoustic impedance and attenuation characteristics of the viscoelastic composites, which formed the basis of the objective function for the design problem. A complex-valued homogenization method was employed to evaluate the effective macroscopic properties of viscoelastic composites, such as their effective impedance and attenuation characteristics, with low computational cost. The homogenization method was incorporated into a density-based topology optimization framework. We formulated the objective functional using the homogenized elasticity tensor and density, and its design sensitivities were calculated using the adjoint variable method.

A numerical example was presented to demonstrate the effectiveness of the proposed method. The results showed that the reflection coefficient cannot be reduced below the performance of the impedance-matching material alone, while the attenuation characteristics exceeded those of the viscoelastic material alone. The optimized structure was composed mostly of impedance-matching material, with the viscoelastic material forming a connected structure. From these results, we conclude that the proposed method is effective for designing viscoelastic composites that minimize reflected and transmitted waves. The optimization outcomes suggest a design guideline: distributing the viscoelastic material as a thin, interconnected lattice within the impedance-matching material is key to achieving the desired acoustic performance.

References

- [1] G. Leventhall, P. Pelmear, S. Benton, A Review of Published Research on Low Frequency Noise and its Effects, Technical Report, Department for Environment, Food and Rural Affairs, UK, 2003. Project Report.
- [2] B. Berglund, T. Lindvall, D. H. Schwela, New who guidelines for community noise, *Noise & vibration worldwide* 31 (2000) 24–29. doi:10.1260/0957456001497535.

- [3] M. Alves-Pereira, N. A. C. Branco, Vibroacoustic disease: biological effects of infrasound and low-frequency noise explained by mechanotransduction cellular signalling, *Progress in biophysics and molecular biology* 93 (2007) 256–279. doi:10.1016/j.pbiomolbio.2006.07.011.
- [4] L. E. Kinsler, A. R. Frey, A. B. Coppens, J. V. Sanders, *Fundamentals of acoustics*, John Wiley & Sons, 2000.
- [5] T. Cox, P. d’Antonio, *Acoustic absorbers and diffusers: theory, design and application*, CRC press, 2016.
- [6] J. Allard, N. Atalla, *Propagation of sound in porous media: modelling sound absorbing materials*, John Wiley & Sons, 2009.
- [7] J. P. Arenas, M. J. Crocker, Recent trends in porous sound-absorbing materials, *Sound & vibration* 44 (2010) 12–18.
- [8] R. S. Lakes, *Viscoelastic materials*, Cambridge university press, 2009.
- [9] J. D. Ferry, *Viscoelastic properties of polymers*, John Wiley & Sons, 1980.
- [10] A. D. Nashif, D. I. Jones, J. P. Henderson, *Vibration damping*, John Wiley & Sons, 1991.
- [11] A. Bensoussan, J.-L. Lions, G. Papanicolaou, *Asymptotic analysis for periodic structures*, volume 374, American Mathematical Soc., 2011.
- [12] E. Sanchez-Palencia, *Non-Homogeneous Media and Vibration Theory*, volume 127 of *Lecture Notes in Physics*, 1 ed., Springer-Verlag Berlin Heidelberg, 1980. doi:10.1007/3-540-10000-8.
- [13] G. Allaire, *Shape Optimization by the Homogenization Method*, volume 146, Springer Science & Business Media, 2012.
- [14] Y.-M. Yi, S.-H. Park, S.-K. Youn, Asymptotic homogenization of viscoelastic composites with periodic microstructures, *International Journal of Solids and Structures* 35 (1998) 2039–2055. doi:10.1016/S0020-7683(97)00166-2.
- [15] M. P. Bendsøe, O. Sigmund, *Topology Optimization: Theory, Methods, and Applications*, Springer Science & Business Media, 2003.

- [16] M. P. Bendsøe, Optimal shape design as a material distribution problem, *Structural optimization* 1 (1989) 193–202. doi:10.1007/BF01650949.
- [17] M. P. Bendsøe, O. Sigmund, Material interpolation schemes in topology optimization, *Archive of Applied Mechanics* 69 (1999) 635–654. doi:10.1007/s004190050248.
- [18] O. Sigmund, On the design of compliant mechanisms using topology optimization, *Journal of Structural Mechanics* 25 (1997) 493–524.
- [19] O. Sigmund, Design of multiphysics actuators using topology optimization—Part I: One-material structures, *Computer Methods in Applied Mechanics and Engineering* 190 (2001) 6577–6604.
- [20] R. Tavakoli, S. M. Mohseni, Alternating active-phase algorithm for multimaterial topology optimization problems: a 115-line matlab implementation, *Structural and Multidisciplinary Optimization* 49 (2014) 621–642. doi:10.1007/s00158-013-0999-1.
- [21] M. P. Bendsøe, N. Kikuchi, Generating optimal topologies in structural design using a homogenization method, *Computer Methods in Applied Mechanics and Engineering* 71 (1988) 197–224. doi:10.1016/0045-7825(88)90086-2.
- [22] K. Suzuki, N. Kikuchi, A homogenization method for shape and topology optimization, *Computer Methods in Applied Mechanics and Engineering* 93 (1991) 291–318. doi:10.1016/0045-7825(91)90245-2.
- [23] O. Sigmund, Materials with prescribed constitutive parameters: an inverse homogenization problem, *International Journal of Solids and Structures* 31 (1994) 2313–2329. doi:10.1016/0020-7683(94)90154-6.
- [24] Y. Noguchi, T. Yamada, Topology optimization of acoustic metasurfaces by using a two-scale homogenization method, *Applied Mathematical Modelling* (2021). doi:10.1016/j.apm.2021.05.005.
- [25] Y. Noguchi, T. Yamada, Level set-based topology optimization for graded acoustic metasurfaces using two-scale homogenization, *Finite Elements in Analysis and Design* 196 (2021) 103606. doi:10.1016/j.finel.2021.103606.

- [26] K.-S. Yun, S.-K. Youn, Multi-material topology optimization of viscoelastically damped structures under time-dependent loading, *Finite Elements in Analysis and Design* 123 (2017) 9–18. doi:10.1016/j.finel.2016.09.006.
- [27] H. Zhang, A. Takezawa, X. Ding, H. Guo, W. Ni, X. Zhang, Topology optimization of composite macrostructures comprising multi-phase viscoelastic composite microstructures for enhanced structural damping, *Composite Structures* 278 (2021) 114712. doi:10.1016/j.compstruct.2021.114712.
- [28] X. Huang, S. Zhou, G. Sun, G. Li, Y. M. Xie, Topology optimization for microstructures of viscoelastic composite materials, *Computer Methods in Applied Mechanics and Engineering* 283 (2015) 503–516. doi:10.1016/j.cma.2014.10.007.
- [29] Q. Liu, D. Ruan, X. Huang, Topology optimization of viscoelastic materials on damping and frequency of macrostructures, *Computer methods in applied mechanics and engineering* 337 (2018) 305–323. doi:10.1016/j.cma.2018.03.044.
- [30] O. Giraldo-Londoño, G. H. Paulino, Fractional topology optimization of periodic multi-material viscoelastic microstructures with tailored energy dissipation, *Computer Methods in Applied Mechanics and Engineering* 372 (2020) 113307. doi:10.1016/j.cma.2020.113307.
- [31] D. Akamatsu, K. Matsushima, T. Yamada, Optimal design of cavity-free mechanical metamaterials exhibiting negative thermal expansion, *International Journal of Mechanical Sciences* 283 (2024) 109693. doi:10.1016/j.ijmecsci.2024.109693.
- [32] F. Hecht, New development in freefem++, *Journal of Numerical Mathematics* 20 (2012) 251–266. doi:10.1515/jnum-2012-0013.